More constraints on internal heating rate of the Earth's mantle from plume observations

Wei Leng[1] and Shijie Zhong[1]

Received 23 October 2008; revised 26 November 2008; accepted 5 December 2008; published 22 January 2009.

[1] Our previous numerical studies of plume dynamics without secular cooling effects demonstrated that the internal heating rate of the Earth's mantle is constrained to be ~70% by inferred plume heat flux and plume excess temperature in the upper mantle. In this paper, by integrating the secular cooling effects into the numerical studies, we demonstrate that the dependence of plume-related observations on internal heating rate is not affected by secular cooling and that the plume-related observations are only dependent on the internal heating rate and insensitive to its partitioning between radiogenic heating and secular cooling, thus confirming the conclusions of ~70% internal heating rate from our previous numerical studies. Furthermore, we present a new analysis to constrain the internal heating rate with the plume-related observations based on the energy balance of mantle convection. The analysis shows that the internal heating rate of the mantle has a lower bound of ~60% to satisfy the energy balance of the mantle with current plume observations, which is consistent with the conclusions from our numerical studies.
Citation: Leng, W., and S. Zhong (2009), More constraints on internal heating rate of the Earth's mantle from plume observations, *Geophys. Res. Lett.*, *36*, L02306, doi:10.1029/2008GL036449.

1. Introduction

[2] The total surface heat flux for the present-day Earth is ~43 TW, among which ~36 TW surface heat flux is attributed to the heat released from mantle convection processes, while the other ~7 TW is caused by radiogenic heating in the continental crust [*Davies*, 1999]. The mantle heat flux consists of three parts: heat from the core, mantle radiogenic heating, and heat loss from mantle secular cooling. The heat loss from mantle secular cooling releases heat from the mantle interior and is similar to the effects of radiogenic heating. These two heating sources are often termed as mantle internal heating. The partitioning of the mantle heat flux among these three heating sources has significant implications for the dynamic evolution and chemical composition of the Earth's mantle and core, but is still under great debates [*Davies*, 1988, 1999; *Sleep*, 1990; *Gubbins et al.*, 2004; *Boyet and Carlson*, 2005; *Huang and Zhong*, 2005; *Sleep*, 2006; *Zhong*, 2006; *Korenaga*, 2008; *Lay et al.*, 2008].

[3] Heat flux from the core may be constrained by studies of mantle plumes that ascend from the Core-Mantle Boundary (CMB) and carry the heat from the core [*Morgan*, 1971]. Plume heat flux in the upper mantle is estimated to be 6%–10% of mantle heat flux or 2.4–3.5 TW, based on observations of plate motion and plume-induced swell topography [*Davies*, 1988; *Sleep*, 1990]. The uncertainties with this estimated plume heat flux may result from temporal and spatial variability of mantle plumes [e.g., *Jellinek et al.*, 2003; *Davies*, 1999]. *Davies* [1988] and *Sleep* [1990] originally treated the plume heat flux in the upper mantle as the heat released from the core, and inferred the mantle internal heating rate to be ~90%. Plume excess temperature in the upper mantle is estimated to be 250–350 K in the upper mantle [*Schilling*, 1991], or 19%–27% of the average temperature in the upper mantle which is generally agreed to be ~1300°C [*Turcotte and Schubert*, 2002]. Numerical modeling of plume dynamics has shown that plume heat flux and plume excess temperature in the upper mantle are strongly dependent on the mantle internal heating rate and that the internal heating rate needs to be ~70% to reproduce the plume-related observations in the upper mantle [*Zhong*, 2006; *Leng and Zhong*, 2008a]. This result triples the estimate of CMB heat flux by *Davies* [1988] and *Sleep* [1990]. The difference is caused by the adiabatic heating effect which significantly reduces plume heat flux as plumes ascend but was ignored by *Davies* [1988] and *Sleep* [1990].

[4] One potential problem from previous numerical studies is that the results are generally quantified after the convection system reaches to a statistically steady state [*Zhong*, 2006; *Leng and Zhong*, 2008a]. The steady-state convection means that there is no secular cooling of the mantle, which may not be appropriate for the Earth's mantle. The secular cooling rate of the mantle is estimated within a large range, from 50–70 K/Ga [*Abbott et al.*, 1994] to ~100 K/Ga [*Nisbet and Fowler*, 1983; *Berry et al.*, 2008]. More studies are therefore needed to verify whether the previous results from steady-state models still stand with secular cooling.

[5] Additionally, the energetics of the mantle requires that the total viscous heating and total adiabatic heating balance out each other [*Turcotte et al.*, 1974; *Hewitt et al.*, 1975; *Zhang and Yuen*, 1996a; *Leng and Zhong*, 2008b], and that the total viscous heating is constrained by surface heat flux and internal heating rate [*Hewitt et al.*, 1975; *Jarvis and McKenzie*, 1980]. On the other hand, from the numerical studies, it has been demonstrated that the plume heat flux is strongly related to the adiabatic heating [*Leng and Zhong*, 2008a]. Based on these arguments, it is natural to ask whether the plume-related observations can be directly used to constrain internal heating rate based on the energy balance.

[1]Department of Physics, University of Colorado at Boulder, Boulder, Colorado, USA.

0094-8276/09/2008GL036449$05.00

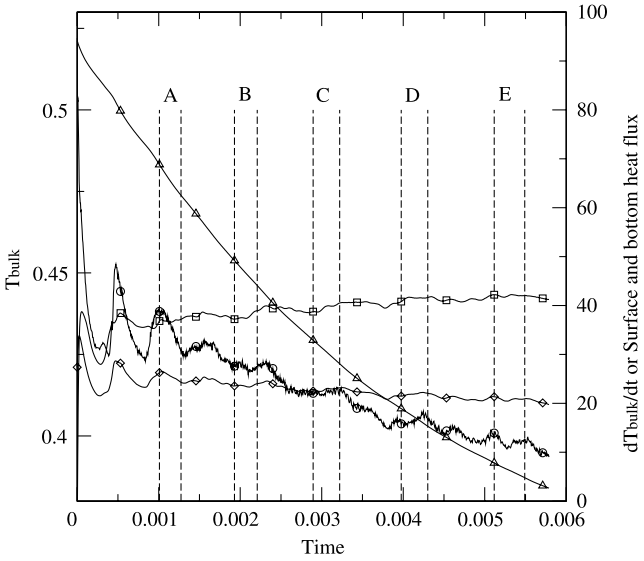

Figure 1. The bulk average temperature T_{bulk} (line with triangles), the change rate of bulk average temperature $\frac{dT_{bulk}}{dt}$ (line with circles), the surface heat flux normalized by surface area (line with diamonds) and the bottom heat flux normalized by bottom area (line with squares) for case SC01 at different time. Periods A–E represent five different time periods that we analyze.

[6] In this paper, we first use numerical models to show that the secular cooling of the mantle does not affect the general conclusions on the relationship between plume dynamics and internal heating rate, thus extending the applicability of our previous results from steady-state convection models. We then present an analysis which demonstrates that the internal heating rate of the mantle can be constrained by plume observations based on energetic balance theorem. Notice that with this method, numerical calculations are no longer necessary in order to constrain the internal heating rate of the mantle. At last, we draw our main conclusions.

2. Plume Dynamics in a Mantle With Secular Cooling

[7] We have formulated new models with secular cooling effects. Our models are similar to those by *Zhong* [2006] and *Leng and Zhong* [2008a]. Basically, we use 3-D regional spherical models CitcomCU to simulate whole-mantle convection with extended Boussinesq approximation. The viscosity in the models is both temperature-dependent (i.e., a factor of 1000 viscosity variation for temperature varying from the surface to the CMB) and depth-dependent (i.e., a factor of 30 viscosity reduction in the upper mantle between 100 km and 670 km depths). We also include 410-km and 670-km phase changes and depth-dependent thermodynamics properties in our models. From the surface to the CMB, the coefficient of thermal expansion decreases by a factor of 5.0 and the thermal diffusivity increases by a factor of 2.18. More details about the models are given by *Zhong* [2006] and *Leng and Zhong* [2008a].

[8] We compute a case SC01 with the secular cooling effects. The Rayleigh number for case SC01 is 4×10^7 and the internal heating parameter H, which represents radiogenic heating, is 18. To simulate the secular cooling effect, we need an initial temperature that is relatively high. We take the steady state temperature from case WM04 by *Leng and Zhong* [2008a] and increase it uniformly by 20% but with the maximum temperature kept as 1.0. The modified temperature field is then taken as the initial condition for case SC01 that is integrated for 550,000 time steps. It should be noted that similar to the Earth, our model is in a mobile-lid convection regime and subducted slabs are continuously generated at the top boundary [*Zhong*, 2006]. After a transition period, the bulk average temperature in case SC01 decreases with time at a stable rate (Figure 1). Notice that the values in Figure 1 are all dimensionless, and for dimensionless time 0.001 is approximately equivalent to 1.3 Ga. Figure 1 also shows the rate of change in the bulk average temperature, $\frac{dT_{bulk}}{dt}$, versus time t. Notice that $\frac{dT_{bulk}}{dt}$ represents the effect of the secular cooling which is quite strong at the beginning, $\sim$40, but is gradually reduced to $\sim$10, comparable to the internal heating parameter H. Surface and CMB heat fluxes of case SC01 also vary with time (Figure 1), suggesting a time dependence of internal heating rate for this case.

[9] We choose five different time periods from case SC01 to quantify plume-related observables and internal heating rates. Each time period includes 30000 time steps, which generally represent 5–10 transit time of the convection system, and the time periods chosen are indicated in Figure 1. Following plume detection and plume analysis techniques by *Leng and Zhong* [2008a], the plume-related values in the upper mantle are quantified and analyzed. Here we are interested in four characteristic values in the upper mantle: plume temperature, T_{p_um}, average mantle temperature, T_{um}, normalized plume heat flux, Q_{p_um}/Q_s, and normalized plume excess temperature, $\Delta T_{plume\_um}/T_{um}$, where Q_{p_um}, ΔT_{plume_um} and Q_s are plume heat flux in the upper mantle, plume excess temperature in the upper mantle, and surface heat flux, respectively. It can be observed that the plume temperature in the upper mantle is nearly constant; the average upper mantle temperature increases with internal heating rate; and the normalized plume heat flux and plume excess temperature in the upper mantle decrease with internal heating rate (Figure 2).

[10] For comparison, we also plot the results of three steady-state cases: WM04–WM06 by *Leng and Zhong* [2008a] in Figure 2. All the model parameters in these three cases are the same as in case SC01, except that the internal heating parameter H varies from 18 to 72. The internal heating rate dependence of plume-related observables and upper mantle average temperature for case SC01 at different time periods follows exactly the same trends as those in statistically steady state cases (Figure 2). In order to reproduce the plume observations, i.e. the shaded zones in Figure 2, the internal heating rate needs to be $\sim$70%. It thus shows that the relations between plume observations and internal heating rate obtained from statistically steady state models [*Zhong*, 2006; *Leng and Zhong*, 2008a] can be applied to the Earth's mantle.

[11] We should point out that in our models the CMB temperature is fixed and that the secular cooling of the Earth's core is not considered. Also, it is possible that the Earth's mantle temperature evolution is not as monotonic as

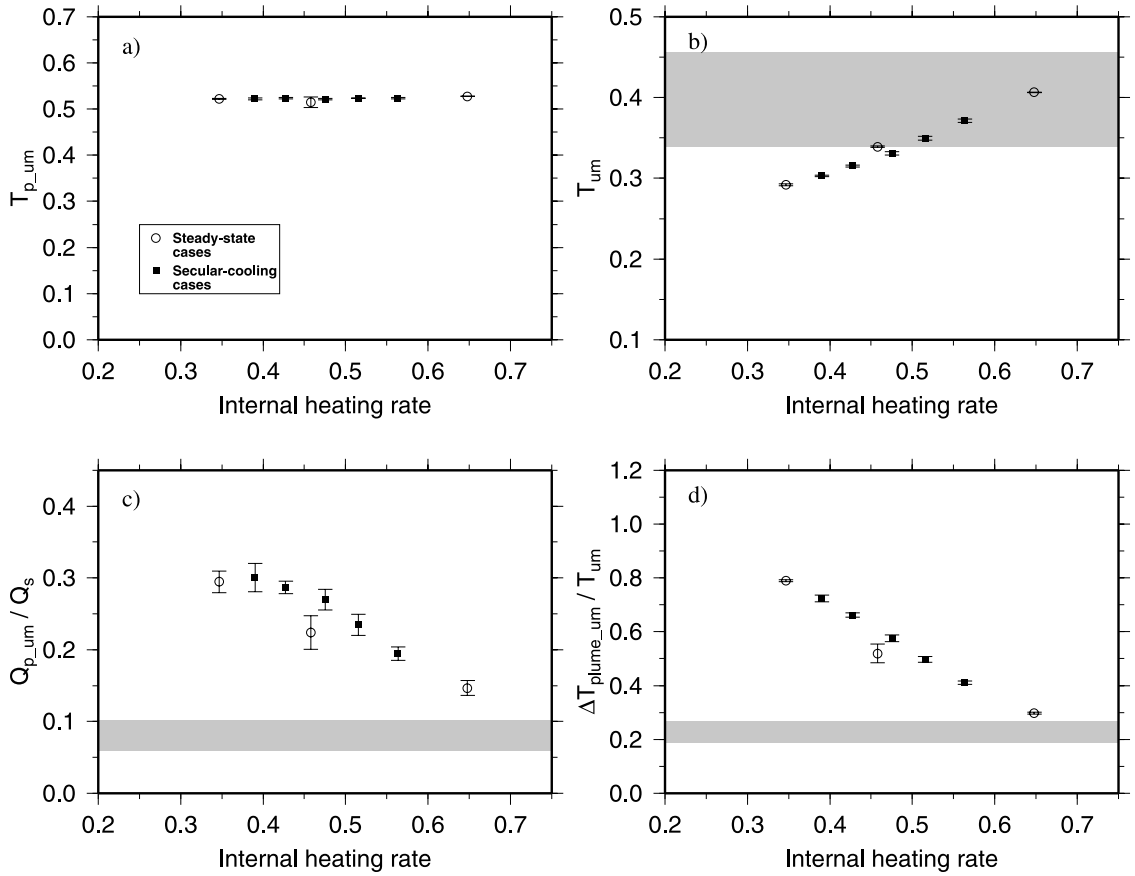

Figure 2. (a) The plume temperature, (b) the mantle average temperature, (c) the normalized plume heat flux and (d) the normalized plume excess temperature in the upper mantle versus internal heating rate. The filled squares represent five different time periods for case SC01, as shown in Figure 1, and the circles represent three cases WM04-WM06 from *Leng and Zhong* [2008a]. The shaded zones indicate the ranges of observations, and the error bars show the standard deviations over the analyzed time periods.

in our simplified models. While it is important for future studies to consider the coupled mantle-core evolution [e.g., *Honda and Iwase*, 1996], we think that our simplified models may still provide important insights into the effects of mantle secular cooling on the plume observations.

3. Constraining Internal Heating Rate of the Mantle From Energy Balance

[12] In a compressible convection system like the Earth's mantle, it has been demonstrated that total viscous heating, Φ, and total adiabatic heating, Q_a, balance out each other at any instant in time, i.e., $\Phi + Q_a = 0$ [*Turcotte et al.*, 1974; *Hewitt et al.*, 1975; *Zhang and Yuen*, 1996a; *Leng and Zhong*, 2008b]. And total viscous heating can be estimated from the surface heat flux, the dissipation number D_i, and the internal heating rate μ as [*Hewitt et al.*, 1975; *Jarvis and McKenzie*, 1980]

$$\Phi \approx D_i(1 - 0.5\mu)Q_s. \tag{1}$$

Dissipation number is defined as $D_i = \alpha g d/C_p$, where α, g, d and C_p are coefficient of thermal expansion, gravitational acceleration, vertical length scale of the convection system and the specific heat at constant pressure, respectively. Both analytical and numerical studies show that equation (1) becomes exact as Rayleigh number is much larger than the critical Rayleigh number [*Hewitt et al.*, 1975; *Jarvis and McKenzie*, 1980]. Equation (1) is derived for a Cartesian geometry from

$$\Phi = \int_V \rho g \alpha T w dV, \tag{2}$$

where ρ, T, w and V are density, temperature, vertical velocity and volume, respectively. For a spherical geometry with inner radius r_i and outer radius r_o, it can be easily demonstrated that equation (2) leads to

$$\Phi = D_i\left(1 - \frac{r_0^3 - (r_0^2 + r_i^2)(r_0 + r_i)/4}{r_0^3 - r_i^3}\mu\right)Q_s. \tag{3}$$

For a planetary mantle with $r_i = 0.55 r_0$, like the Earth's mantle, the coefficient before μ is 0.594.

[13] Previous studies have revealed that the distribution of the viscous heating and adiabatic heating are strongly localized [*Bercovici et al.*, 1992; *Balachandar et al.*, 1995; *Zhang and Yuen*, 1996b; *Tackley*, 1996]. Viscous heating mostly concentrated in top and bottom thermal boundary layers, and in regions surrounding plume and slab areas as

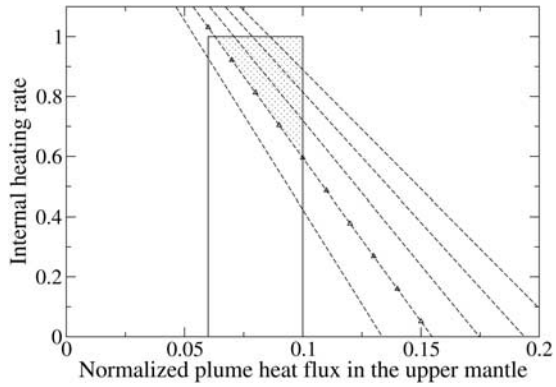

Figure 3. The internal heating rate constrained by the normalized plume heat flux and the normalized plume excess temperature in the upper mantle. Obtained from inequality (9), the five dashed lines show the lower bounds of internal heating rate for the normalized plume excess temperature of 16%, 19%, 22%, 25% and 28% (from bottom to top). The solid-line box indicates the observed range of plume heat flux, 6%–10%. Considering the observed range of plume excess temperature, 19%–27%, the dashed line with overlapped triangles and the solid-line box together constrain the range of internal heating rate to be within the dotted zone. The lower bound of the internal heating rate is ~60%.

well, while significant adiabatic heating occurs only in plume and slab regions where vertical motions are intense. Viscous heating is always positive, while adiabatic heating is negative for upwelling plume regions and positive for downwelling slab regions. Suppose that Q_{a_p} and Q_{a_s} are the adiabatic heating for plume regions and slab regions, respectively, we have

$$\left|Q_{a\_p}\right| = |Q_a - Q_{a\_s}| > |Q_a| = \Phi. \tag{4}$$

On the other hand, adiabatic heating for plume regions can be related to plume observations in the upper mantle. Plume heat flux in the upper mantle, Q_{p_um}, can be expressed as

$$Q_{p\_um} = M\Delta T_{plume\_um} = M\left(T_{p\_um} - T_{um}\right), \tag{5}$$

where M is plume mass flux. In order to relate upper mantle plume heat flux to the adiabatic heating in plume regions, we need to make two assumptions. The first one is that the plume mass flux is a constant as plumes ascend from near the CMB to the upper mantle; the second one is that the adiabatic heating in plume regions is the dominant factor to cool the plumes during their ascending. Considering the small viscosities and the large vertical velocities in plume regions, these two assumptions are justified as demonstrated in our numerical studies [*Leng and Zhong*, 2008a]. With these two assumptions, the adiabatic heating for plume regions, Q_{a_p}, causes plume temperature T_p to decrease adiabatically. At two different radii r_1 and r_2 in the mantle, plume temperature follows its own adiabat [*Leng and Zhong*, 2008a],

$$\frac{T_p(r_1)}{T_p(r_2)} = e^{\gamma D_i \Delta r}, \tag{6}$$

where γ is the ratio of the Earth's radius to the mantle thickness, and $\Delta r = r_2 - r_1$. Numerical modeling of plume dynamics by *Leng and Zhong* [2008a] showed that plume temperature is consistent with the predictions by equation (6). Given that the adiabatic heating in plume regions is the dominant factor to cool the plumes, we have

$$Q_{a\_p} = -M\left(T_{p\_cmb} - T_{p\_um}\right), \tag{7}$$

where T_{p_cmb} is the plume temperature above the CMB. Substituting equation (6) into equation (7) leads to

$$Q_{a\_p} = -M\left(T_{um} + \Delta T_{plume\_um}\right)\left(e^{\gamma D_i \Delta r} - 1\right). \tag{8}$$

Combining equation (3), (4), (5) and (8), we obtain an inequality

$$\mu > \frac{1}{0.594}\left[1 - \frac{1}{D_i}\frac{Q_{p\_um}}{Q_s}\left(1 + \frac{T_{um}}{\Delta T_{plume\_um}}\right)\left(e^{\gamma D_i \Delta r} - 1\right)\right]. \tag{9}$$

From inequality (9), the internal heating rate of the mantle has a lower bound determined by the plume-related observations including normalized plume excess temperature and normalized plume heat flux in the upper mantle. This lower bound decreases with D_i and normalized plume heat flux, but increases with normalized plume excess temperature. Δr in inequality (9) is taken as 0.35, which excludes the top and bottom thermal boundary layers where the plumes are not well defined and the adiabatic heating is negligible. D_i for the Earth's mantle is approximately 0.7. With the given Δr and D_i, Figure 3 shows how the lower bound of the internal heating rate depends on different plume heat flux and plume excess temperature. From Figure 3, the current ranges of plume heat flux and plume excess temperature in the upper mantle together constrain the internal heating rate of the mantle to be within the dotted region. In other words, the minimum internal heating rate of the mantle is ~60%. This lower bound is achieved when the normalized plume heat flux and normalized plume excess temperature are 10% and 19%, respectively. If we vary the D_i between 0.6 and 0.8, the lower bound of the internal heating rate generally varies less than 5%.

[14] This analysis provides an independent confirmation of our previous conclusions based on numerical models that the internal heating rate of the mantle needs to be ~70% to reproduce the plume-related observation [*Zhong*, 2006; *Leng and Zhong*, 2008a].

4. Conclusions

[15] We have formulated models of plume dynamics with secular cooling effects. We demonstrate that the plume observations in the upper mantle are dependent on the internal heating rate of the mantle, and are insensitive to how the internal heating is partitioned between the radiogenic heating and the secular cooling. These results corroborate the conclusions from our previous studies which do not include the effects of secular cooling. Furthermore, based on the energy balance of mantle convection and using the plume-related observations, we present an analysis

that provides a lower bound on the internal heating rate of the mantle. This analysis, which is independent from our previous numerical models, indicates that the internal heating rate of the mantle is larger than 60%, which is consistent with the conclusions from our previous numerical studies.

[16] **Acknowledgments.** This study is supported by National Science Foundation and David and Lucile Packard Foundation.

References

Abbott, D., L. Burgess, J. Longhi, and W. H. F. Smith (1994), An empirical thermal history of the Earths upper mantle, *J. Geophys. Res.*, *99*, 13,835–13,850.

Balachandar, S., D. A. Yuen, D. M. Reuteler, and G. S. Lauer (1995), Viscous dissipation in three-dimensional convection with temperature-dependent viscosity, *Science*, *267*, 1150–1153.

Bercovici, D., G. Schubert, and G. A. Glatzmaier (1992), Three-dimensional convection of an infinite-Prandtl number compressible fluid in a basally heated spherical shell, *J. Fluid Mech.*, *239*, 683–719.

Berry, A. J., L. V. Danyushevsky, H. C. O'Neill, M. Newville, and S. R. Sutton (2008), Oxidation state of iron in komatiitic melt inclusions indicates hot Archaean mantle, *Nature*, *455*, 960–963.

Boyet, M., and R. W. Carlson (2005), 142Nd evidence for early (>4.53 Ga) global differentiation of the silicate Earth, *Science*, *309*, 576–581.

Davies, G. F. (1988), Ocean bathymetry and mantle convection: 1, *Large-scale flow and hotspots, J. Geophys. Res.*, *93*, 10,467–10,480.

Davies, G. F. (1999), *Dynamic Earth: Plates, Plumes and Mantle Convection*, 458 pp., Cambridge Univ. Press, New York.

Gubbins, D., D. Alfè, G. Masters, D. Price, and M. Gillan (2004), Gross thermodynamics of 2–component core convection, *Geophys. J. Int.*, *157*, 1407–1414.

Hewitt, J. M., D. P. McKenzie, and N. O. Weiss (1975), Dissipative heating in convective flows, *J. Fluid Mech.*, *68*, 721–738.

Honda, S., and Y. Iwase (1996), Comparison of the dynamic and parameterized models of mantle convection including core cooling, *Earth Planet. Sci. Lett.*, *139*, 133–145.

Huang, J., and S. Zhong (2005), Sublithospheric small-scale convection and its implications for the residual topography at old ocean basins and the plate model, *J. Geophys. Res.*, *110*, B05404, doi:10.1029/2004JB003153.

Jarvis, G. T., and D. P. McKenzie (1980), Convection in a compressible fluid with infinite Prandtl number, *J. Fluid Mech.*, *96*, 515–583.

Jellinek, A. M., H. M. Gonnermann, and M. A. Richards (2003), Plume capture by divergent plate motions: Implications for the distribution of hotspots, geochemistry of mid-ocean ridge basalts, and estimates of the heat flux at the core-mantle boundary, *Earth Planet. Sci. Lett.*, *205*, 361–378.

Korenaga, J. (2008), Urey ratio and the structure and evolution of Earths mantle, *Rev. Geophys.*, *46*, RG2007, doi:10.1029/2007RG000241.

Lay, T., J. Hernlund, and B. A. Buffett (2008), Core-mantle boundary heat flow, *Nature Geosci.*, *1*, 25–32.

Leng, W., and S. Zhong (2008a), Controls on plume heat flux and plume excess temperature, *J. Geophys. Res.*, *113*, B04408, doi:10.1029/2007JB005155.

Leng, W., and S. Zhong (2008b), Viscous heating, adiabatic heating and energetic consistency in compressible mantle mantle convection, *Geophys. J. Int.*, *173*, 693–702.

Morgan, W. (1971), Convection plumes in the lower mantle, *Nature*, *230*, 42–43.

Nisbet, E. G., and C. M. R. Fowler (1983), Model for Archean plate tectonics, *Geology*, *11*, 376–379.

Schilling, J. G. (1991), Fluxes and excess temperatures of mantle plumes inferred from their interaction with migrating midocean ridges, *Nature*, *352*, 397–403.

Sleep, N. H. (1990), Hotspots and mantle plumes: Some phenomenology, *J. Geophys. Res.*, *95*, 6715–6736.

Sleep, N. H. (2006), Mantle plumes from top to bottom, *Earth Sci. Rev.*, *77*, 231–271.

Tackley, P. J. (1996), Effects of strongly variable viscosity on three-dimensional compressible convection in planetary mantles, *J. Geophys. Res.*, *101*, 3311–3332.

Turcotte, D. L., A. T. Hsui, K. E. Torrance, and G. Schubert (1974), Influence of viscous dissipation on Benard convection, *J. Fluid Mech.*, *64*, 369–374.

Turcotte, D. L., and G. Schubert (2002), *Geodynamics*, 2nd ed., 456 pp., Cambridge Univ. Press, New York.

Zhang, S., and D. A. Yuen (1996a), Various influences on plumes and dynamics in time-dependent, compressible mantle convection in 3-D spherical shell, *Phys. Earth Planet. Inter.*, *94*, 241–267.

Zhang, S., and D. A. Yuen (1996b), Intense local toroidal motion generated by variable viscosity compressible convection in 3-D spherical-shell, *Geophys. Res. Lett.*, *23*, 3135–3138.

Zhong, S. (2006), Constraints on thermochemical convection of the mantle from plume heat flux, plume excess temperature, and upper mantle temperature, *J. Geophys. Res.*, *111*, B04409, doi:10.1029/2005JB003972.

W. Leng and S. Zhong, Department of Physics, University of Colorado at Boulder, Boulder, CO 80309, USA. (wei.leng@colorado.edu)